

**Development of Advanced Surface Enhancement Technology
for Decreasing Wear and Corrosion of Equipment
Used for Mineral Processing**

ANNUAL TECHNICAL PROGRESS REPORT

(July 21st, 2003 – July 21st, 2004)

Dr. Daniel Tao
Department of Mining Engineering, University of Kentucky
234E, MMRB, Lexington, KY 40506-0107

Dr. Craig A. Blue
Oak Ridge National Laboratory
P.O. Box 2008 MS6083
Oak Ridge, TN 37831-6083

DE-FC26-03NT41787

August, 2004

**University of Kentucky Research Foundation
201 Kinkead Hall, Lexington, KY 40506-0057**

**Oak Ridge National Laboratory
P.O. Box 2008 MS6083, Oak Ridge, TN 37831-6083**

DISCLAIMER

This report was prepared as an account of work sponsored by an agency of the United States Government. Neither the United States Government nor any agency thereof, nor any of their employees, makes any warranty, express or implied, or assumes any legal liability or responsibility for the accuracy, completeness, or usefulness of any information, apparatus, product, or process disclosed, or represents that its use would not infringe privately owned rights. Reference herein to any specific commercial product, process, or service by trade name, trademark, manufacturer, or otherwise does not necessarily constitute or imply its endorsement, recommendation, or favoring by the United States Government or any agency thereof. The views and opinions of authors expressed herein do not necessarily state or reflect those of the United States Government or any agency thereof.

ABSTRACT

Equipment wear is a major concern in the mineral processing industry, which dramatically increases the maintenance cost and adversely affects plant operation efficiency. In this research, wear problems of mineral processing equipment including screens, sieve bends, heavy media vessel, dewatering centrifuge, etc., were identified. A novel surface treatment technology, high density infrared (HDI) surface coating process was proposed for the surface enhancement of selected mineral processing equipment. Microstructural and mechanical properties of the coated samples were characterized. Laboratory-simulated wear tests were conducted to evaluate the tribological performance of the coated components. Test results indicate that the wear resistance of AISI 4140 and ASTM A36 steels can be increased 3 and 5 folds, respectively by the application of HDI coatings.

TABLE OF CONTENTS

INTRODUCTION	1
EXECUTIVE SUMMAR	11
EXPERIMENTAL	13
Materials	13
HDI Coating Preparation	14
Sample Characterization	16
REDULTS AND DISCUSSION	19
Microstructure	19
Microhardness	28
Wear Testing	30
CONCLUSIONS	34
REFERENCES	35

INTRODUCTION

Mineral processing is the science of separating valuable minerals from the gangue minerals out of ores to produce basic materials such as coal, quartz, salt, copper and gold that are used in the industry and everyday life. The mineral processing industry deals with a very large tonnage of mineral ores and products. Equipment wear happens inevitably, which increases the equipment maintenance costs and plant downtime and reduces the process efficiency of the plant. Wear is believed to be one of the most significant problems in the mineral processing industry. It is estimated that up to 40% operating costs of a mineral processing plant are caused by equipment maintenance (Laurila and Budge, 2000).

During the last two decades, significant efforts have been made to reduce wear of cyclones, heavy medium vessel, pipe lines and pumps which are widely used in mineral processing. The goal has been realized by using the ceramic linings to coat the inner surface of the high wear equipment (Foster, 1996). The different shapes of ceramic linings are installed inside the vessels and cyclones, which are much harder and have stronger wear resistance. They can greatly increase the lifetime of mineral processing equipment (Nonnen et al., 1985).

However, research has not been effectively performed to reduce the wear of screens, chains for conveyors and pug mill paddles for coal mixing, which have to be replaced very often as a result of wear. Due to size and complex geometry of screen, it is not feasible to apply ceramic lining to the screen. As the screen wears, the screen openings will become wider and wider. During this process, the screen loses the consistency of aperture and reduces the screening efficiency. The increased screen openings also reduce the efficiency of downstream operations due to non-ideal feed to them. Furthermore, the replacement of screens will increase the plant shutdown time and reduce the overall plant efficiency. The development of advanced surface enhancement technology and its application to screens and other equipment to enhance their wear lives are strongly desired by the mining and mineral processing industry.

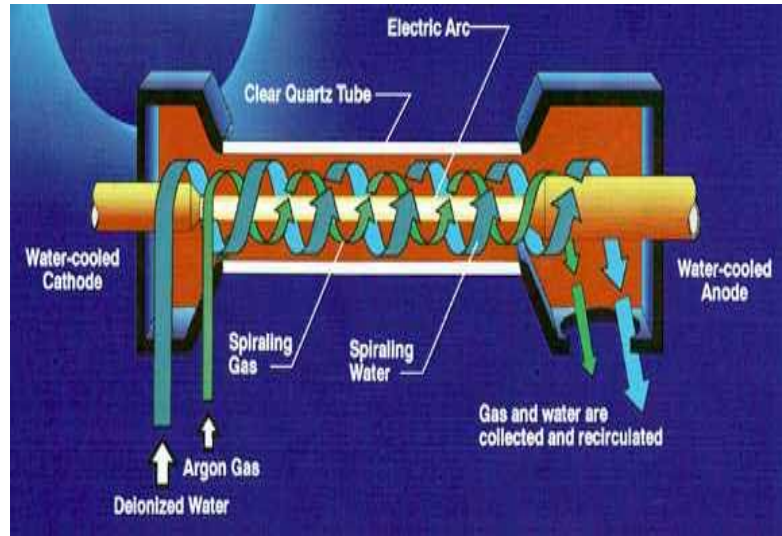


Figure 1. Schematic of plasma arc lamp

High-Density Infrared (HDI) process is a novel technology developed by the Oak Ridge National Laboratory (ORNL). This process involves producing infrared heating with extremely high power densities of up to 3.5 kW/cm^2 using a unique plasma arc lamp (PAL) system. The lamp is schematically shown in Figure 1.

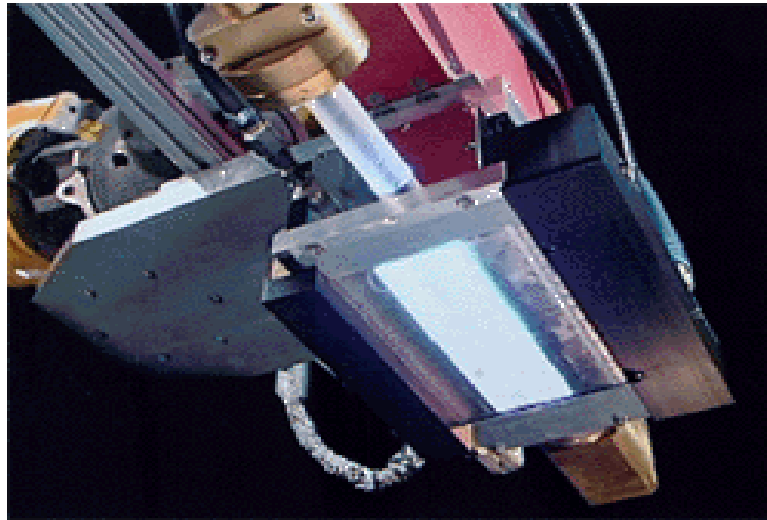


Figure 2. Plasma arc lamp

The lamp, as shown in Figure 2, consists of a quartz tube of 3.175 cm in diameter and 10.16 cm, 20.32 cm or 38.1 cm in length. The lamp is sealed at the ends where the cathode and anode are located. Deionised water mixed with argon or nitrogen gas enters at the cathode side through high velocity jets impinging at a given angle. Due to the high velocity and pressure, the water is then impelled to the wall of the quartz tube and spirals down the length of the tube in a uniform film of 2-3 mm thick. This water film serves two purposes: to cool the quartz wall and to remove any tungsten particulates that may be

expelled from the electrodes. The gas moves in a spiral fashion through the center of the tube, and a capacitive circuit initiates the plasma which has a temperature in excess of 10,000 K, is stable and produces a radiant spectrum of 0.2-0.4 μm . The plasma is absorbed by metal surfaces with high efficiency. The powder coatings of wear resistant materials are also highly absorbing, because the open areas act like black bodies. Figure 9 shows an actual plasma-infrared lamp used at ORNL.

Infrared heating is an inherently clean, noncontact heating method that provides rapid-response energy fluxes capable of heating rates in excess of 3000° C/s, rapid power-level changes, high cooling rates and a controllable temperature-gradient. Coating materials are fused by the PAL, yielding metallurgical bonding between coating and substrate. It was demonstrated that the method could fuse and metallurgically bond coatings and steel substrates without convective mixing, providing a new means for the rapid thermal processing of surface coatings (Engleman et al., 2002). It has been applied to the treatment of metals (Blue et al., 2000; Muralidharan et al, 2004). HDI surface treatment process has been successfully applied in the wear parts used for bulldozers manufactured by the Caterpillar Inc. More than 5-fold of wear enhancement has been achieved (Blue, 2002).

One of the projects at ORNL using the plasma-arc lamp is to develop coatings for casting dies used to make aluminum auto parts. The dies are fitted with AISI Type H13 hot-work tool steel pins used to form holes in the cast part so they don't have to be machined in, which reduces manufacturing costs. The dies are placed in an H-13 steel housing. When liquid aluminum is injected into the dies, it reacts with the H-13 steel, degrading it and gradually making the die unusable.

Using the plasma source, tools are coated with a chromium-carbide coating that protects H-13 steel from attack by liquid aluminum. The plasma lamp is used to precisely and rapidly heat the precursor material on the H-13 steel, making coatings that fuse with the substrate without changing the base material properties. Because the intense radiant heating sets up large temperature gradients so fast, the iron in the H-13 steel has almost no time to dissolve. Thus, heat treating of the coated component is not necessary. Advantages of using a plasma radiant source to fuse coatings include:

- Large area coverage (3.175×35 cm in a line focus and up to 10×20 cm in a uniform irradiance)
- No convective mixing of coating material with the base material
- Rapid cooling of coating material
- Minimal effects on base material
- No degradation of carbide reinforcements in coating
- No temperature limitation (can readily melt tungsten - melting point = 3410° C)

Wear- and corrosion-resistant coatings, such as tungsten carbide and chromium carbide, fused to a part substrate could be useful in rolling mills and in the chemical process and heavy equipment such as mining and mineral processing industries.

Wear in Mineral Processing

Mineral processing usually includes several unit operations, including comminution, classification/screening, concentration/processing and post-treatment (e.g., product dewatering). Wear occurs in every stage of the process. The equipment wear problems that exist in each of the aforementioned processes are discussed as follows:

Comminution is referred to as the gradual reduction of a hard mineral to a fine powder by crushing or grinding for direct use or further processing. This includes liberation of a product, such as coal from non-coal material. It also includes primary crushing, where run-of-mine ore is reduced to a size small enough to feed a secondary crusher and rock is broken down to an adequate size for grinding. Mineral comminution, especially grinding, requires large energy costs and may account for more than half of hard rock processing energy costs (Wills, 1985). According to the mining annual review conducted by the Mining Journal (1999), approximately 29 billion kWh of electrical energy is consumed each year for size reduction. Therefore, wear issues associated with this energy intensive process of comminution have been extensively studied and many approaches, from optimizing the equipment design to the development of wear resistant materials, have been adopted during the past two decades (Durman, 1988; Norman, 1980). The wear issues regarding comminution equipment is beyond the scope of this research.

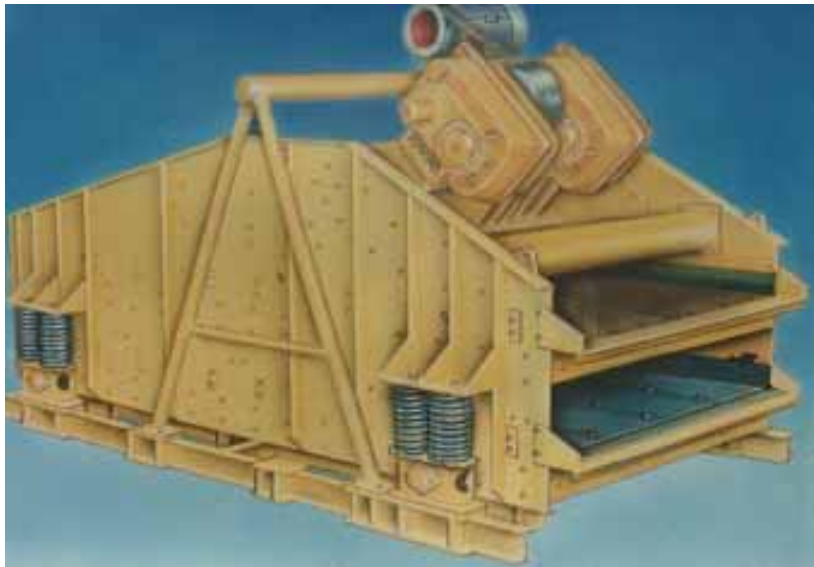


Figure 3. A typical vibrating screen for raw coal screening

Screen (Figure 3) is the most commonly used device in the mineral processing industry to separate particles by size. Modern mineral processing would not be possible without efficient screening. In a coal processing plant, screening accomplishes sizing by passing coal of different sizes through a series of screens, each of a decreasing size. The

individual screen discharges are then directed into different screen products for subsequent processing or sale. In processing industry, screens are also used for product dewatering, heavy media recovering, etc. (Leonard and Hardinge, 1991). During screening process, the aperture increases as material wears, resulting in inconsistent aperture sizes and lower screening efficiency because more oversize particles may report to the underflow, which as a result creates non-ideal feed to the downstream processes.



Figure 4. Sieve bend

Sieve bend (Figure 4) is another high capacity screening device widely used for fine particle ($150\ \mu\text{m} \sim 3\ \text{mm}$) classification. Coal slurry is fed tangentially to the concave surface of a sieve bend, which provides a centrifugal force that presses the feed liquid layer against the screen surface. A shaving of liquid is formed due to the centrifugal force together with a retardation of the fluid velocity next to the screen (caused by frictional drag). Therefore, the particle classification is achieved when the shaved liquid enters the open slots and reports to the underflow stream. During fine particle classification, the bar between two adjacent slots of a sieve bend becomes rounded due to wear. Most sieve bends are made of stainless steels, and the wear life of most surface screens is usually between 1,000 and 2,000 hours of operation. Frequent replacement results in high maintenance costs.

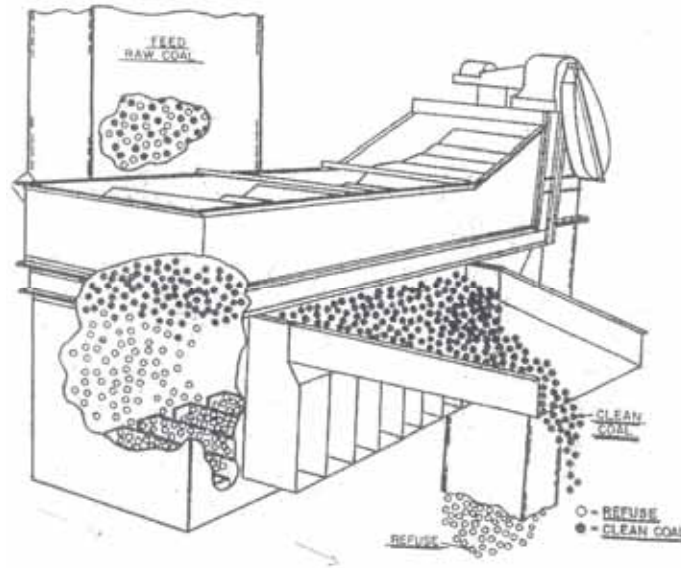


Figure 5. Schematic of a dense medium vessel

Concentrating is the process of separating valuable minerals from their ores using the physical or physico-chemical property differences of different components. There are many mineral concentrating processes used in the coal and mineral processing industry. Dense medium separation process is the most widely used coal processing method, which accounts for 49% of the processing units used worldwide (Laurila, 1998). There are two types of dense medium separators in mineral processing, which are dense medium cyclone and dense medium vessel, as shown in Figure 5. Since ceramic linings have been developed and commercially used in dense medium cyclones to protect their inner walls (Foster, 1996), the wear enhancement of dense medium cyclones will not be covered in this research. It should be noted that the wear issues concerning heavy medium vessels which accounts for 26.3% of the coal preparation units in the United States (Laurila, 1998) have not been well addressed. In a heavy medium vessel, a feed sink plate is usually used to direct the feed (raw coal and dense medium suspension) downward into the vessel so that particles do not raft across the width of the bath. Thus, the plate is subject to high wear as the feed slides down along the plate into the vessel.

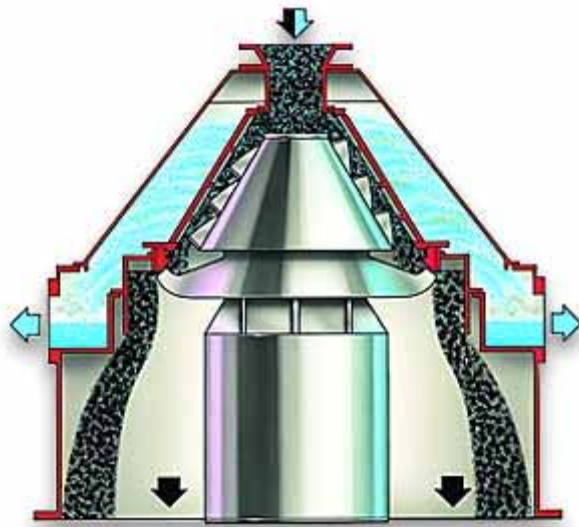


Figure 6. Schematic of a dewatering centrifuge

The purpose of product dewatering is to control the post-processed product, e.g., clean coal, to an acceptable moisture level. Centrifuge is commonly used in the coal preparation and mineral processing industry for product dewatering. A typical perforate-basket centrifuge is schematically shown in Figure 6. Centrifuges achieve separation by means of the accelerated gravitational force achieved by a rapid rotation. The separation is similar in principle to that achieved in a gravity separation process. The driving force is higher because it is resulting from the rotation of the liquid, unlike gravity sedimentation, where the driving force is from the difference in density between the solid particles and the liquid. The centrifuge separation is achieved with a force 1000 to 20000 times of the gravity. The centrifuge screen is subjected to wear when particles are pressed against the screen surface due to the high centrifugal force generated by the fast rotation.

It should be mentioned that the literature survey conducted by the author indicated that the equipment wear issue in mineral processing has not been well addressed. In the past, research efforts have been mostly focused on the wear problems of the energy-intensive comminution equipment. Little work has been done on the study of wear enhancement of screening, heavy medium vessel and dewatering equipment. Although the energy consumption of these devices is much lower than that of the comminution equipment, wear deteriorates the separation performances of these devices and, as a result, affects the overall plant process efficiency is affected.

Wear Mechanism Analysis

Screen and Sieve Bend

Screens can classify a broad range of sizes and are used for various applications throughout the coal preparation plant, including raw coal pre-treatment and dry fines extraction, pre-sizing of feeds to separation processes, recovery and dewatering of

products after separation processes and sizing of washed coal to meet market requirements. To simplify the discussion, only raw coal pretreatment screens are studied.

In a coal preparation plant, vibrating screens are usually employed for raw coal pretreatment process. Coal particles are fed onto the screen deck at a given speed (e.g., 10 ~ 20 cm/s in the Big Creek Coal Prep Plant, Sidney, KY). The particles then either pass through or remain on the screen deck, resulting in wear of the panel surface. In the meantime, the screen deck itself vibrates vertically to improve the probability for undersize coal particles to pass through the screen and report to the undersize product stream. Coal particles bounce up and down on the panel surface as they travel down to the discharge end, which leads to impact wear when particles hit the screen panel. Therefore, screen wear in the real world consists of both sliding and impact wear. However, the vibrating amplitude of a raw coal screen is usually within 3 ~ 5 millimeters, thus sliding wear still dominates during screening process.

Figure 7 shows a replaced steel screen panel from the Big Creek Coal Prep Plant. It can be observed that the feed end where coal contacts the screen first became very thin after a period of time. The panel could not support the load when it becomes thin. Therefore, the wear resistance of this location should be paid special attention to get extended service life. One possibility is, if surface coating is to be applied on the screen surface, a relative strong coating should be applied on the feed end. This can be achieved by changing the coating process parameters or use of different coatings on the same panel.



Figure 7. A replaced raw coal screen panel

Figure 8 presents a close-up image of a replaced screen panel. The opening size of this screen was 2" × 5/8". After a period of time, the apertures were distorted along the direction of coal flow (black arrow in the figure), and opening size was enlarged by wear, which results in more oversize materials reporting to the underflow. This creates non-ideal feed to the downstream processes and therefore deteriorates the plant process

efficiency. Also, it is found that the wires between two successive apertures are vulnerable to wear. This is because when coal particles slide on the deck, they will unavoidably hit these wires. On the other hand, the near size particles can be stuck at this position, yielding a problem called “blinding.” With the continuous attack from the coal particles or blinding, the wires become thin and they may even break after a period of time. Thus, this should be another concern for the coating development.

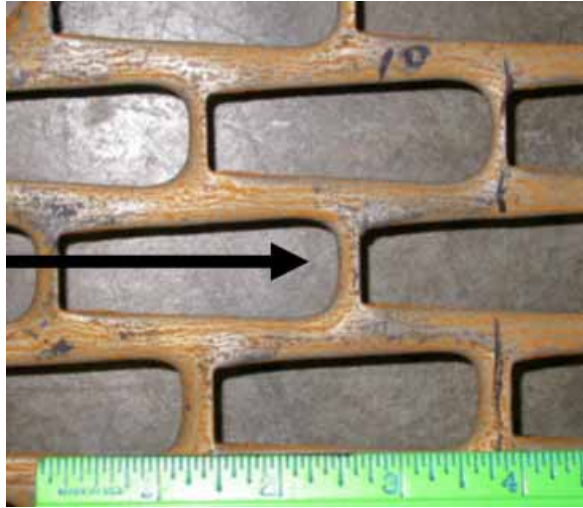


Figure 8. Close-up of a failed screen pane

Sieve bend is constructed as an arc or bend. Wear occurs on the screen bars when feed slurry enters the bend surface tangentially. As discussed previously, sliding wear exists on sieve bend.

Side Plate of Heavy Medium Vessel

Coal particles and heavy medium suspension which is a mixture of water and fine magnetite are fed to the vessel through the slide plate. Wear happens when the feed slides down on the surface of the slide plate. Thus, the slide plate is subjected to abrasive wear.

Dewatering Centrifuge

Similarly, the screen centrifuge is subjected to sliding wear as coal particles rotates tangentially along the screen surface.

Besides, sliding wear is believed to be dominating factor in the wear of banana screen panels, sieve bends and centrifuge screens, and abrasive wear is the main reason for the failure of heavy medium vessel side plate. Wear in mineral processing equipment is a complex system in wear sliding wear is only one contributing component. For most mineral processing equipment, wear caused by abrasion and impact can not be overlooked.

In the reality, there does not exist a clear border between abrasive and sliding wear. Abrasive wear occurs at any mechanical device when involves the motion of bulk solids relative to the surface. Normally, the bulk solid velocities are quite low, with pure sliding taking place, for example in the process of screening. Abrasive wear rates for steels and irons generally increase with increase mineral hardness (Dunn, 1985). Watson and co-workers (1980) found that rapid improvement in metal abrasion resistance when the metal hardness (H) to abrasive hardness (Ha), H/H_a , is greater than 0.6. For a specific mineral processing process, the abrasive hardness can not be changed, thus, the use of coatings with high hardness is recommended as a measure to improve the lifespan of the abrasive wear parts.

It should be mentioned that for an abrasive wear process to happen, the abrasive particles produce parallel grooves on the metal surface while the particles move along on the surface. Metal is cut away from the plastically displaced by ploughing furrow along the path of the abrasive bodies. This explains the wear mechanism of abrasive wear that occurs in mineral processing.

In contrast to abrasive wear, impact wear occurs when materials drop to the metal surface with high velocity. Therefore, there exists the kinetic energy conversion in an impact process. The energy of the impact particles either is transferred to other particles or is dissipated in forms of heat and damaging the metal surfaces of the equipment, resulting in cracks, plastic deformation, cutting or removal of the metal components.

EXECUTIVE SUMMARY

This project is aimed at developing advanced surface enhancement technology for decreasing the wear and corrosion rate of mineral processing equipment by an order of magnitude. The proposed process is expected to be easily adaptable to automation and less expensive than currently used methods. Such performance improvement will result in energy savings of 2.45×10^{14} Btu/year. Significant efforts have been directed toward reducing wear of cyclones, pumps, heavy medium vessels, etc. used in mineral processing during the last two decades or so. Major progress has been achieved through the use of ceramic linings that have considerably increased the lifetime of hydrocyclones. However, little has been done to reduce the wear of screens, chains for conveyors, and piping where ceramic lining is impractical. The screen aperture increases as material wears, resulting in inconsistent aperture sizes and lower screening efficiency. This creates non-ideal feed to downstream operations, reducing their efficiencies. The wear of pipes, particularly the joint elbows, is another major concern of plant operators. The combination of corrosion and wear severely impacts the life span of chains, especially pin, bushings, and side plates. For horizontal conveyor systems, current materials used for chains include chrome-plated pins in an effort to minimize the combined wear/corrosion issues. However, stress-corrosion issues of chain components are continual problems. For inclined systems, corrosion issues are more limited; however, significant wear issues remain. Frequent replacements of screens, conveyors, and pipes increase equipment downtime and maintenance cost and reduce process efficiency. The development of advanced surface enhancement technology is of great interest for the mineral processing and coal preparation industry.

HDI coating technology has been successfully applied to surface enhancement of mineral processing components. Two substrate materials of AISI 4140 steel and ASTM A36 screen sections, and two coating materials of (Ni-10P)-60WC and Fe-15Cr-14Mo-2Y-15C-6B, wt% were investigated. High density infrared (HDI) coating technology was adopted to process the coatings on the substrate. Two passes of fusing current including 200A, 300A, 400A and 600A for preheating pass and 600A, 700A, 725A, 750A, 800A and 900A for fusing pass were applied to achieve the coatings with different characteristics. After the HDI process, specimens were prepared for a series of characterization studies, including optical microscopy and scanning electron microscopy for the microstructural examination, microhardness testing for hardness characterization, and finally the block-on-disk wear tests to measure the wear performance of the HDI processed coating. The following conclusions can be drawn from the results obtained from the study during the first year:

- Surface coatings with refined microstructural features were obtained by using HDI coating process.
- SEM characterization showed the HDI coatings were metallurgically bonded to the substrates.
- The hardnesses of both WC and amorphous coatings are higher than that of substrate materials. The hardness of WC coating was up to three times higher than that of AISI 4140 steel and amorphous coating also achieved a three times higher hardness with the ASTM A36 steel.

- Sample A3, coated with (Ni-10P)-60WC on AISI 4140 steel by HDI (10 mm/s, 300A/700A), showed the best wear resistance in the WC coating group. The wear resistance increased up to 5 times compared to uncoated AISI 4140.
- The EDS analyses showed the presence of WC particle and WC rich-phase. The hard WC coatings significantly enhanced wear resistance of substrate AISI 4140 steel.
- Of three amorphous coatings, Sample B2 coated with amorphous coating Fe-15Cr-14Mo-2Y-15C-6B, wt%, on AISI 4140 steel by HDI (10 mm/s, 400A/800A) showed the best wear resistance. The wear life of AISI 4140 steel increased about 3 times by this amorphous coating.
- For screen substrate, Sample Y3 coated with amorphous coating Fe-15Cr-14Mo-2Y-15C-6B, wt%, by HDI (10 mm/s, 800A) had the best wear resistance. The wear life of this coated materials increased about 5 times than the uncoated screen.
- High porosity was observed with most HDI-processed coatings which adversely affected coating performance, e.g., Sample Y1, Y2 etc.

EXPERIMENTAL

Materials

Two steels were selected as substrates in this research, which are AISI 4140 and ASTM A36, respectively. AISI 4140 is one of the chromium, molybdenum, manganese low alloy steels noted for high toughness, good tensile strength as well as high fatigue strength. It is widely used in fabrication of equipment used in the mineral processing industry. ASTM A36 is widely used for framing and general structural purposes to provide strength and stability. Also, the screen panels studied in this research are made of this steel. The chemical compositions of AISI 4140 and ASTM A36 are listed in Tables 1 and 2, respectively (Davis, 1998).

Table 1. Chemical compositions of the AISI 4140 steel (in wt.%)

Element	C	Mn	P	S	Si	Mo	Cr	Fe
Weight, %	0.38 - 0.43	0.75 - 1.00	0.035 (max)	0.04 (max)	0.15 - 0.30	0.15 - 0.25	0.8 - 1.10	Bal.

Table 2. Chemical composition of ASTM A36 steel (in wt. %)

Element	C	P	S	Si	Cu	Fe
Weight, %	0.25	0.04	0.05	0.4	0.2	Bal.

The mineral processing industry requires materials having strength, toughness, wear and corrosion resistance. It should be noted that coating steels using high energy process such as laser with ultrahard ceramic particles has been developed to meet the extreme requirements of wear, oxidation and corrosion resistance (Agarwal, 2000; Khedkar et al, 1997). As a result, metallurgically sound interface between the coating and the substrate can be formed. However, as the physical properties such as thermal expansion coefficient (CTE) between the ceramic and the steels usually are different, cracks usually develop at the ceramic/steel interface as well as within the coating during the rapid solidification and cooling progress (Agarwal et al., 2000). The use of binders in coating materials can promote the good adhesion between the coatings and the steel substrates. For example, iron has been revealed as an excellent binder for Ti-based coatings on steels (Raghunath et al., 1995). Ni-P binder was used by Engleman and co-workers (2002) to coat WC on AISI 4340 steel using HDI.

Based on the experience accumulated by ORNL researchers, a range of coating materials will be employed for both HDI and LSE processes. These materials include Fe-based amorphous materials (Fe-15Cr-14Mo-2Y-15C-6B, wt%), Thermite (Fe_3O_4 -34.4Al,

wt %), WC, Ti-based ceramics (TiC, TiB₂), etc. In the present investigation, Ni-P binder was used for the preparation of ceramic coatings on steels.

HDI Coating Preparation

Sample-Pretreatment

Test samples were cut to a suitable size (3"×3") for coating preparation. Each specimen was pre-treated prior to coating preparation. This involves removing any grit stuck in the sample surface by using grit blasting and wire brushing. The sample then was wiped down with acetone to remove any residual oils etc. followed by rinsing with alcohol to remove the residual from the acetone.

Coating Preparation

The hood was set up for spraying which includes lining hood with blotter paper, turning on blowers, assembling spray gun and hooking up regulator for spray gun. Then coating precursor powders are mixed and LISI 1008 is added to proper consistency for spraying. The then slurry is shook to make it well suspended and homogenized. The as-prepared coating slurry is transferred to a Venturi effect spray gun and sprayed coating evenly over the specimen.

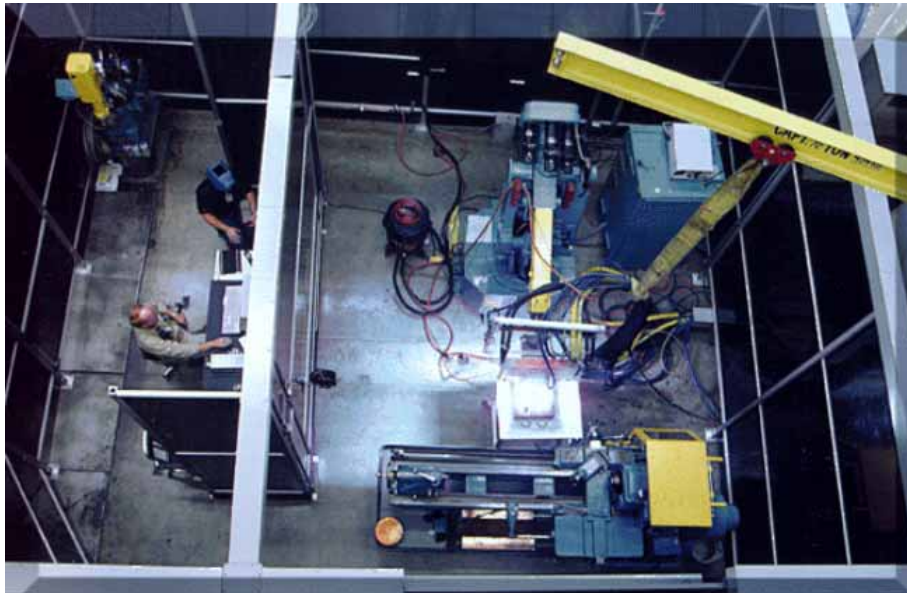


Figure 9. HDI facility at ORNL

To some extent, coating development is a trial and error procedure. In order to achieve the greatest benefits of the proposed technology, process parameters will have to be optimized. HDI is a relatively new surface treatment method. Based on the known experiences, variables that can be adjusted for HDI operation include infrared intensity, surface enhancement through heat treatment with and without external additions, coating

material, coating thickness, coating method, infrared dwell time, etc. After processing parameters were determined, the specimen was placed under the computer-controlled HDI lamp for processing. Figure 9 shows an overview of the HDI facility at ORNL.

Table 3. HDI process parameters for Sample A1-A3 and B1-B3

Sample	Substrate Materials	Coating Materials	Scanning Speed, mm/s	Current, A	
				Preheating pass	Second pass
S	AISI 4140	Uncoated	N/A	N/A	N/A
A1	AISI 4140	40(Ni-10P)-60WC	10	300	750
A2	AISI 4140	40(Ni-10P)-60WC	10	300	725
A3	AISI 4140	40(Ni-10P)-60WC	10	300	700
B1	AISI 4140	Amorphous	10	600	800
B2	AISI 4140	Amorphous	10	400	800
B3	AISI 4140	Amorphous	10	300	800

Table 4. HDI process parameters for Sample Y1, Y2 and Y3

Sample	Substrate Materials	Coating Materials	Scanning Speed, mm/s	Current, A	
				Preheating pass	Second pass
T	Screen section	Uncoated	N/A	N/A	N/A
Y1	Screen section	Amorphous	10	N/A	900
Y2	Screen section	Amorphous	10	200A	600
Y3	Screen section	Amorphous	10	N/A	800

In the past year, a considerable amount of tests were designed and performed to find the “ideal” HDI-treated coating. For the convenience of presentation, a reduced dataset was reported in this report. This includes the test results from 9 typical coupons including 6 AISI 4140 steel coupons denoted as A1 to A3 and B1-B3, and 3 ASTM A36 steel coupons (Y1-Y3), i.e., raw coal screen sections. For the purpose of comparison, an untreated AISI 4140 and an ASTM A36 coupon were also involved. The processing parameters of each specimen are listed in Tables 3 and 4, respectively.

Sample Characterization

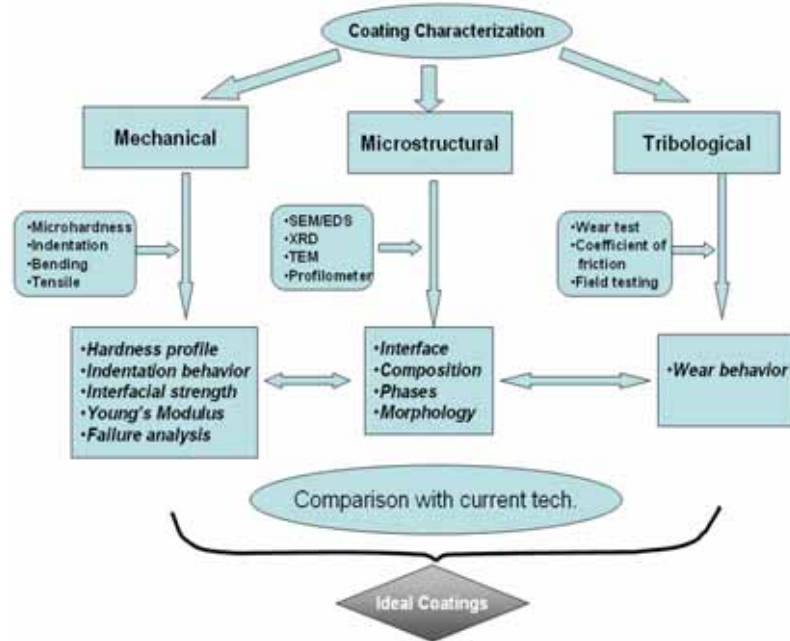


Figure 10. Coating characterization

The characterization work is to investigate the mechanical, microstructural as well as tribological properties of processed specimens. A flowsheet for coating characterization is shown in Figure 10.

The scope of microstrural characterization includes observation the bonding of the coating/substrate interface, phase distribution in the coating system. The specimens were cut from each sample by NIABRAZE CBN circular abrasive saw and a Buehler Isomet 11-1180 low speed diamond saw. The specimens were then mounted using epoxy resin with cross-section of coating-substrate interface exposed outside. The resin mounted specimen was easy to handle and ensured that the exact cross-section surface should be polished. The mounted specimens were polished by mechanical grinding with a series of sand papers from coarse to fine (labeled with the following numbers: 200, 400, 600, 800, 1000 and 1200 grits). The purpose of this procedure was to remove the damages produced during cutting process. After the specimens were ground over the finest sand paper, the final step was to finish up on a polishing cloth with 0.3 μm alumina paste to obtain scratch free surfaces. This step was to remove any scratches or damage generated by the grinding. Figure 11 shows a typical prepared specimen for SEM microstructure examination which was cut from Sample A1, then mounted and polished to get scratch free surface.

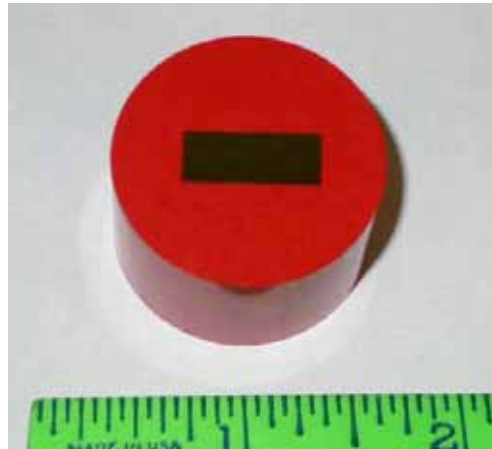


Figure 11. A typical specimen prepared for SEM study

The scratch free specimen surfaces were then etched to reveal the grain structure of the metallic phases. 2% Nital (98 ml ethanol + 2 ml nitric acid) was used as the etchant. The etchant did two things to the specimen surface. First, it chemically removed the deformed thin layer on the surface which was produced during the polishing process. Second, the etchant selectively attacked the highest energy sites on the surface without affecting the others. As a result, different crystal orientations, grain boundaries, precipitates, phases and defects were showed distinctly under the microscopy for the microstructure investigation. A Hitachi S-3200 scanning electron microscope (SEM, Figure 12) equipped with energy dispersive spectroscopy (EDS) was employed to perform the microstructural characterization.



Figure 12. Hitachi S-3200 SEM

The mechanical properties was be examined by microindentation from which coating hardness profile can be achieved. Microindentation behavior of the coating and

substrate will be studied at different loads. Figure 13 shows the indentation instrument (Micro Photonics, Irvine, CA), used in this research.

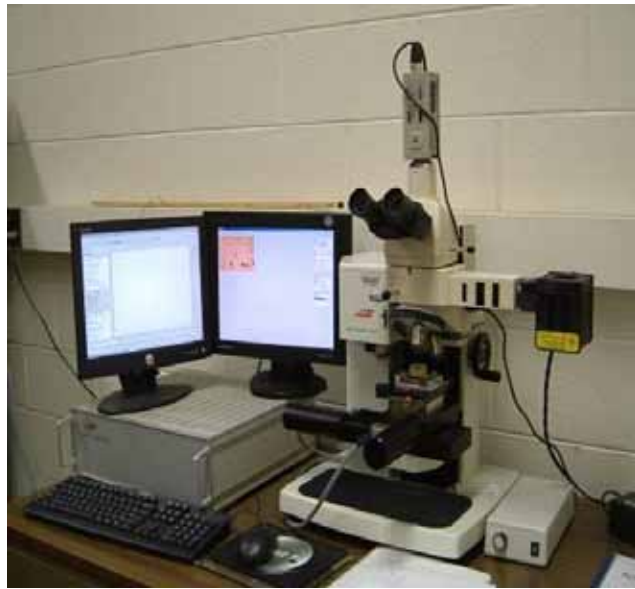


Figure 13. Microindentation tester

The wear resistance of HDI-treated specimens was tested in lab using an in-house constructed block-on-ring wear test machine. Each coated specimen will be slid against a hardened tool steel ring (HRC \approx 60, D = 82 mm). The ring's rotating speed is controlled at 1000 ± 20 rpm. Specimen weight loss was measured after each successive 2 minutes for a total test duration of 20 minutes. A normal load of 10 lbs (4.54 kg) will be applied on the specimen during the test. The test principle is schematically shown in Figure 14.

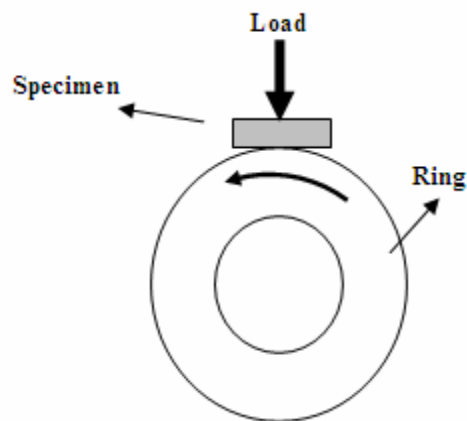


Figure 14. Schematic of block-on-ring wear test

RESULTS AND DISCUSSION

Microstructure

Optical Microscopic Studies

The microstructure of each sample was investigated using optical microscopy, SEM and analyzed by EDS method. Figures 15 and 16 show the cross section images of Sample A1 to A3 and B1 to B3, which were taken by optical microscopy (OM). Sample A1, A2 and A3 were WC coatings prepared by the HDI process. The common characteristic of the three coatings is that their thickness is relatively small. The coating thickness is not uniform along the interface for each of Sample A1, A2 and A3.

The rest of the samples, B1 B2 and B3 are all amorphous coatings prepared by HDI. It seems all the coatings were metallurgically bonded to the substrate. More detailed structure information would be revealed on the SEM images. It can be seen that the coatings were unevenly adhered to the substrates. Coating on Sample B1 was not continuously bonded with substrate. Sample B2 had a relatively thick coating compared with Sample B1 and B3.

For Sample B1 and B3, it can also be found that the upper part of each coating is more even than its bottom part. This can be explained by the different reaction intensities between the coating and substrate, i.e. higher reaction intensity results in deeper penetration of the coating to the substrate layer. But even for the same coupon surface, the reaction intensity is not uniform for different locations which can lead to structure heterogeneity of coatings.

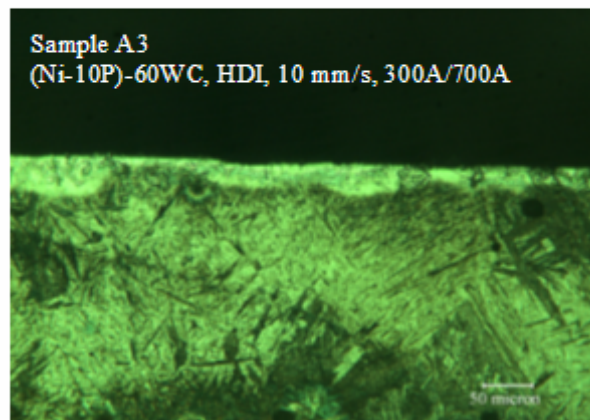
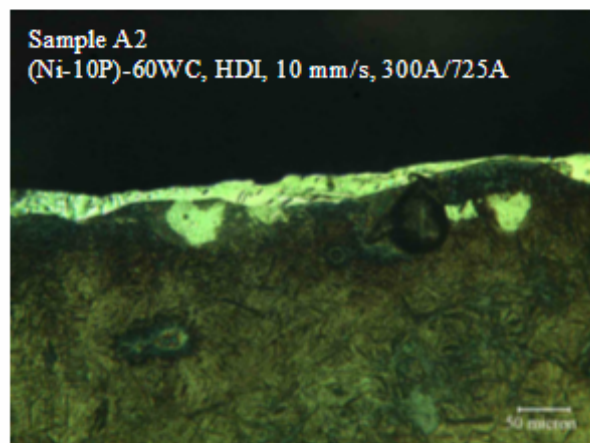
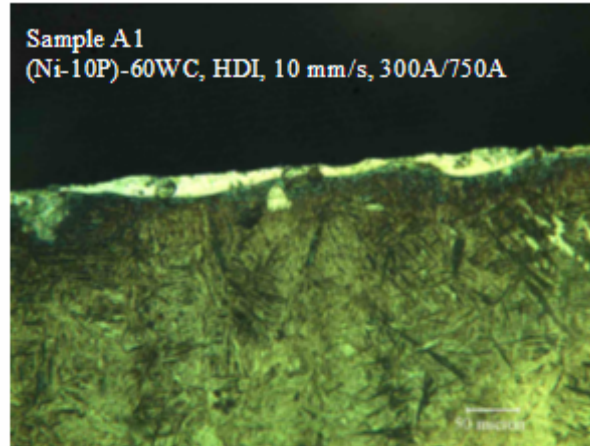


Figure 15. OM images for Sample A1, Sample A2 and Sample A3

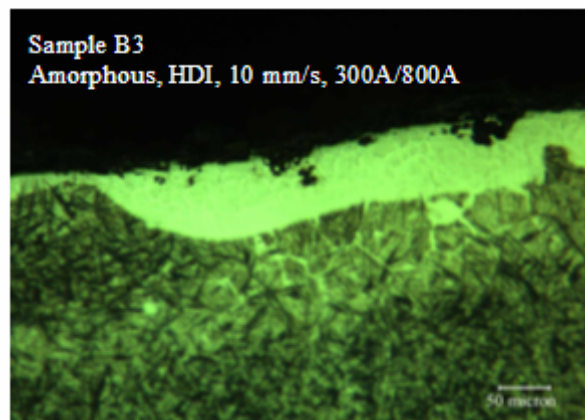
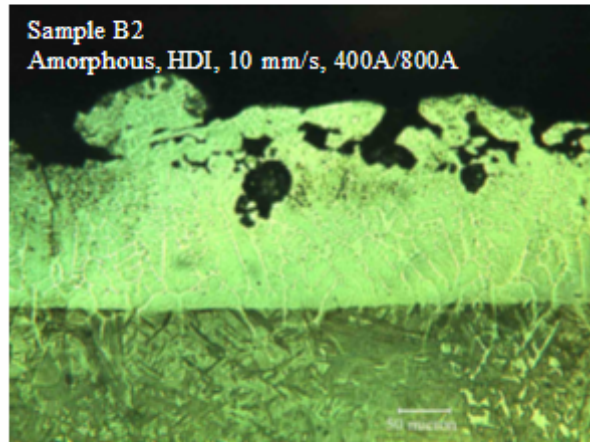
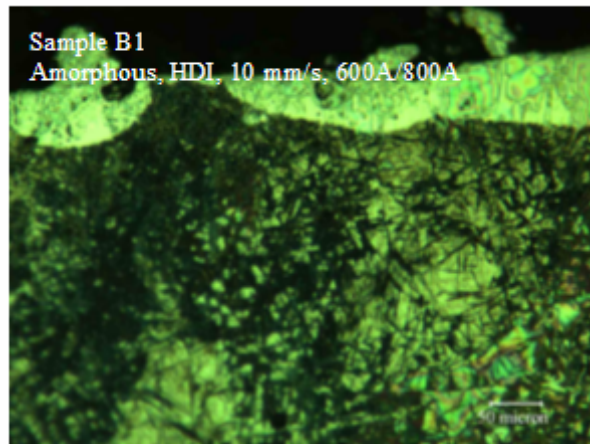


Figure 16. OM images for Sample B1, Sample B2 and Sample B3

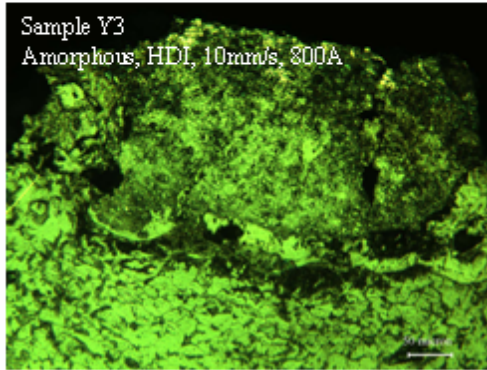
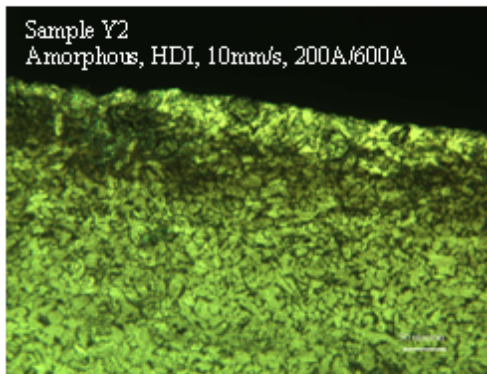
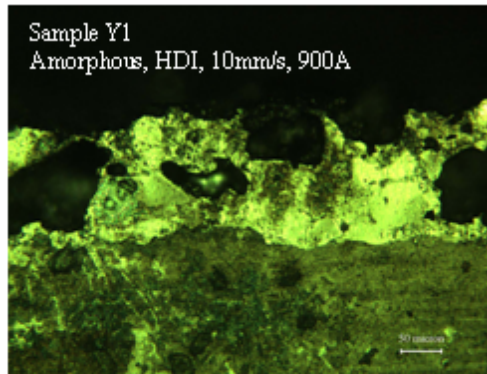


Figure 17. OM images of Sample Y1, Y2 and Y3

Figure 17 shows optical microscope images of screen section samples Y1, Y2 and Y3. with amorphous coatings. It is clear that Sample Y1 had more pores than Sample Y2 and Sample Y3. The distinct interface between coating and substrate can be seen in Sample Y1, which means the bonding was weak and the coating was easy to peel off. Sample Y2 and Sample Y3 had relatively uniform coating and no coating-substrate boundary.

SEM Characterization

SEM examinations were carried out to further investigate the microstructures of coatings and substrates. The cross section SEM morphologies of Sample A1 to A3 and B1 to B3 are shown in Figures 18 and 19. As you can see from each SEM image, there are three regions marked as coating, interface (or heat affected zone) and substrate. During the HDI process, the materials located near the substrate-coating interface had metallurgical reactions to form some new materials as a result of the heat flux of the PAL which did not exist either in the substrate or coating before the process. The presence of heat affected zone with certain depth proved that the coatings were metallurgically bonded to the substrates. Generally, poor bonding between coating and substrate always degrades the coating adhesion strength. As a result, the coating may detach easily from the substrate, damaging its mechanical and tribological performance. The strong metallurgical bonds are known to significantly increase the coating-substrate adhesion strength.

In Figure 18, many bright islands were observed. These precipitations were agglomerate WC particles which were confirmed by EDS analysis. The WC particles sunk toward the bottom of the coating. Wu et al. (1995, 2004) also reported similar results. This phenomenon can be explained by the significant difference in the density between WC (15.6 g/cm^3) and Ni-P (8.2 g/cm^3). During the solidification of the transient coating, the heavier WC particles precipitated towards the bottom and formed the WC rich phase (the bright cluster). Another reason is Ni-P based materials melted faster than WC due to its low melting point under the high temperature processing conditions. WC particles melted relatively slow or even partially melted at beginning stage of the process. That's why WC particles had the tendency to stay at the bottom of the molten metal.

For the Iron-based amorphous coatings (Figure 19), the distinct observation was that the coating thickness was higher than that of WC coatings. The coating of Sample B2 had the thickness of about $250 \text{ }\mu\text{m}$. There are some pores seen under SEM or even under low magnifications microscopy. The pores were initiated by thermal spraying prior to HDI process. During the thermal spraying, powders of coating material were sprayed onto the substrate. A lot of "splats" and "voids" were formed. The pores observed under the microscope can be in the form of trapped air or vacuum. In the subsequent step of the HDI process, some voids coalesced and collapsed. Some voids in the form of air were just trapped in the bulk materials. The splats were not always completely fused, which caused some defects and voids in the final coatings. It should be noted that the pores are weakest spots and can cause corrosion on the surface as a result of attack by some

chemicals (Ahn et al., 2004). The direct effect of increased coating porosity is the reduction in coating density. In consequence it may damage the coating performance.

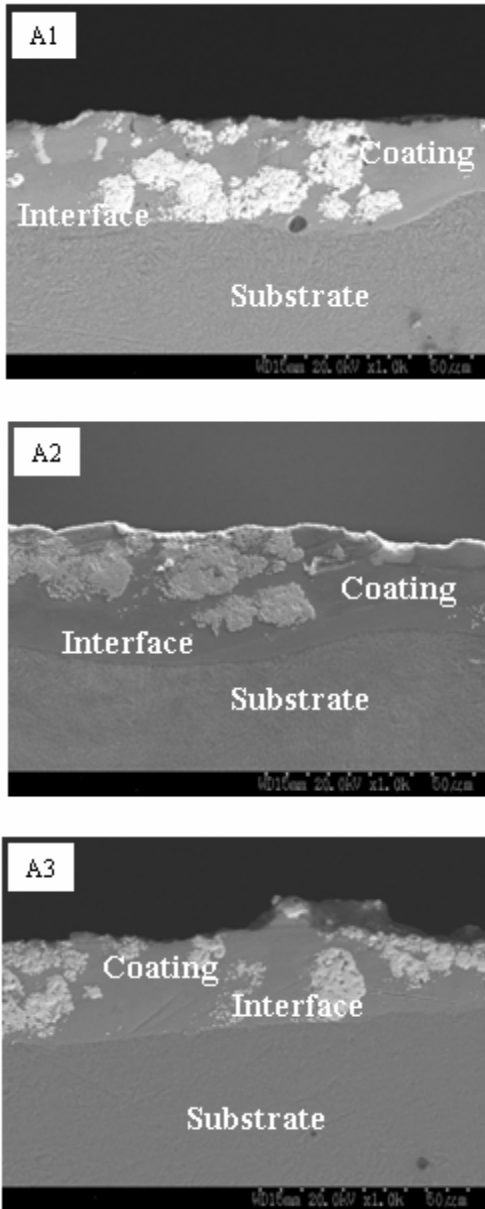


Figure 18. SEM images for Sample A1, Sample A2 and Sample A3

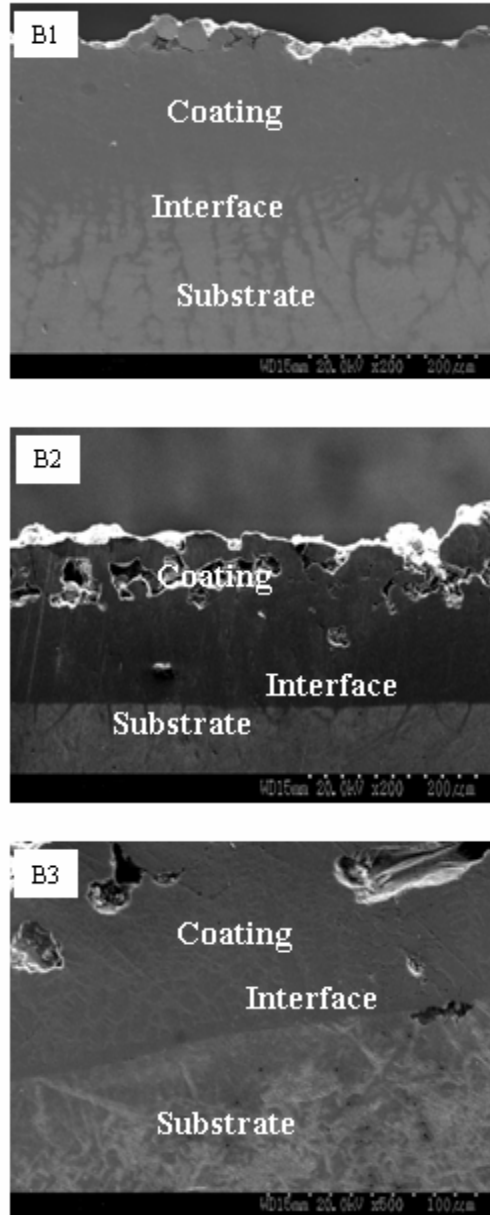


Figure 19. SEM images for Sample B1, Sample B2 and Sample B3

Figure 20 shows the SEM images of Sample Y1, Y2 and Y3 that were obtained to further investigate the microstructure of the coatings. The three regions named as coating, interface and coating were observed. The substrate and the coating were metallurgically bonded. But both Sample Y1 and Sample Y2 had high porosity. The pores are the weakest regions in the coating and are susceptible to corrosion attack. When the abrasive wear happens, the coating with high porosity is loose and tends to show a faster wear rate. The coating of Sample Y3 was more uniform and no large pores were observed. Based on the visual observation, the quality of Sample Y3 coating was much better than that of Sample Y1 and Y2.

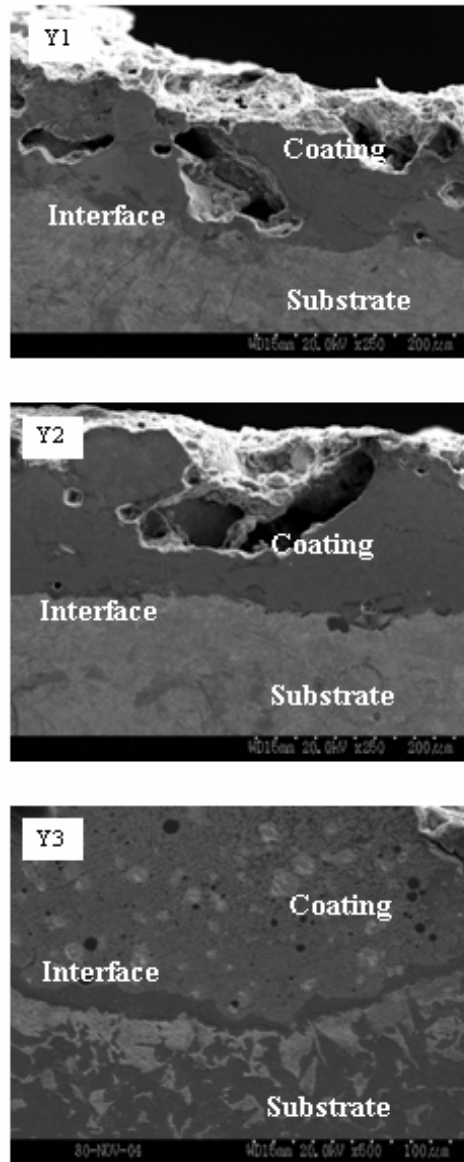


Figure 20. SEM images of Sample Y1, Y2 and Y3

EDS Measurements

EDS analysis was performed at different depths of coating and substrate to examine their elemental compositions. Figure 21 gives the EDS result of the substrate materials, AISI 4140 steel. The peaks obtained are very close to the standard AISI 4140 compositions (Table 1), except that the peaks for Mo were not detected in our study.

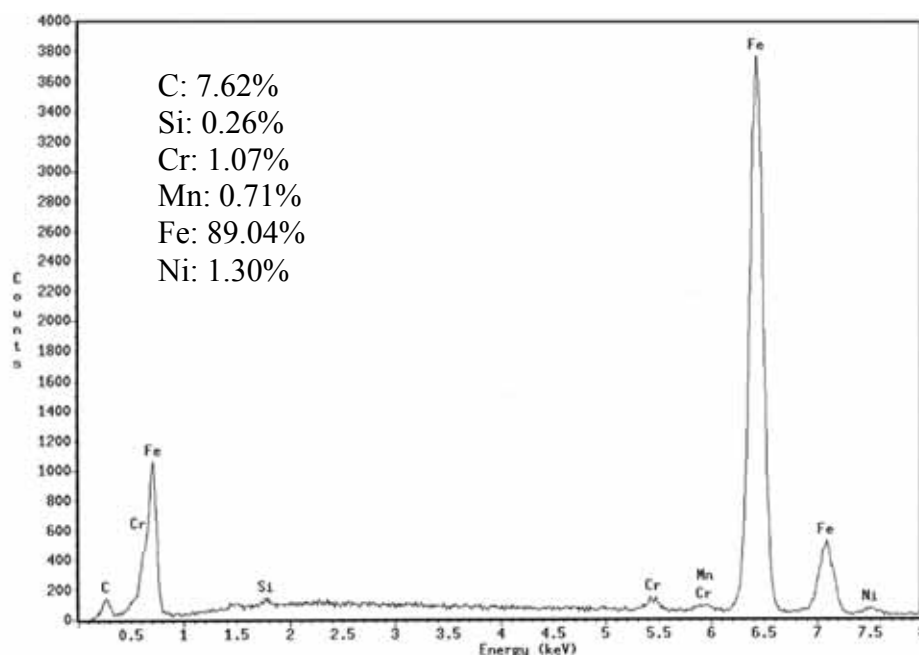


Figure 21. The EDS result of AISI 4140 steel

EDS tests were also performed on all the coatings to investigate elemental distribution in the coatings. For the white clusters in Sample A1, A2 and A3 with WC coatings, high content of tungsten element was detected in the EDS results. The data in Table 5 further indicate that tungsten and carbon are the main compositions in the white islands, which confirmed that those white phases were partly dissolved or precipitated WC particles. The presence of Fe was due to the dissolution of Fe from AISI 4140 steel substrates and small amount of Ni came from the Ni-P binder in the powder precursor.

Table 4. EDS results for WC rich cluster

Sample	C, wt%	Fe, wt%	Ni, wt %	W, wt%
A1	11.09	12.87	1.76	74.27
A2	8.12	9.56	3.94	78.38
A3	9.58	2.36	0.95	87.12

EDS analyses were conducted in the non-WC rich areas (the coating matrix) to show the general element distribution in the coatings. The EDS results are listed in Table 6. In the non-WC rich area, the higher content elements were Fe and Ni.

Table 5. EDS results for the Matrix of WC coatings

Sample	C, wt%	Fe, wt%	Ni, wt%	W, wt%
A1	6.86	61.94	25.49	4.55
A2	8.93	55.80	24.17	3.21
A3	8.94	40.42	33.75	2.36

It can be found from Table 6 that in the three specimens with WC coatings, high content of iron existed in the coating matrix. However, the iron was not included in the precursor powder before coating processing. The explanation for the presence of iron element in coating matrix is that Fe diffused rapidly in the coating. During the HDI process, the coating became liquid when fused by powerful plasma arc lamp. A thin layer of substrate materials melted under the heat flux of the PAL and Fe diffused from the substrate to the coating. The non-consistent element distribution means that coating regrouped itself during the HDI process, generating different phases. The hard WC precipitations may act as reinforced phases and increase the wear resistance of the coating.

Table 6. EDS results for amorphous coatings

Sample	C, wt%	Fe, wt%	Cr, wt%	Mo, wt%
B1	7.84	84.85	3.69	1.85
B2	9.47	67.88	10.37	11.81
B3	8.3	77.16	7.22	5.92

Table 7 shows the element compositions of Sample B1, B2 and B3. In the three amorphous coatings, typical elements of iron-based coating such as Cr and Mo were detected. The content of iron increased from 50% in the coating precursor to around 70% in the final coating, which must be migrated from substrate materials during the HDI process. The contents of Cr and Mo decreased compared with powder precursor.

Microhardness

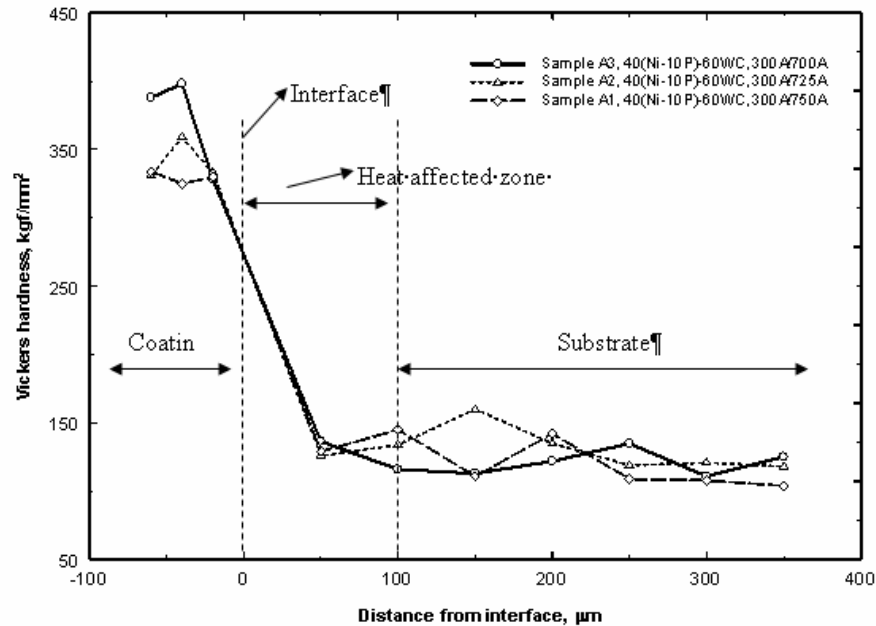


Figure 22. Microhardness profile of Sample A1, A2 and A3

The microhardness tests were performed with a Vickers microhardness tester. The Vickers hardness values were calculated using the load and the diagonal length of the

indent. The microhardness profiles of Sample A1, A2 and A3 are shown in Figure 22 which illustrates that the microhardness of coating was much higher than that of AISI 4140 steel substrate. It was very obvious that the coating processed by HDI technology increased the surface hardness of the materials. As shown in Figure 22 for the three WC coatings, Sample A3 exhibited the highest microhardness which is about four times higher than that of the substrate materials.

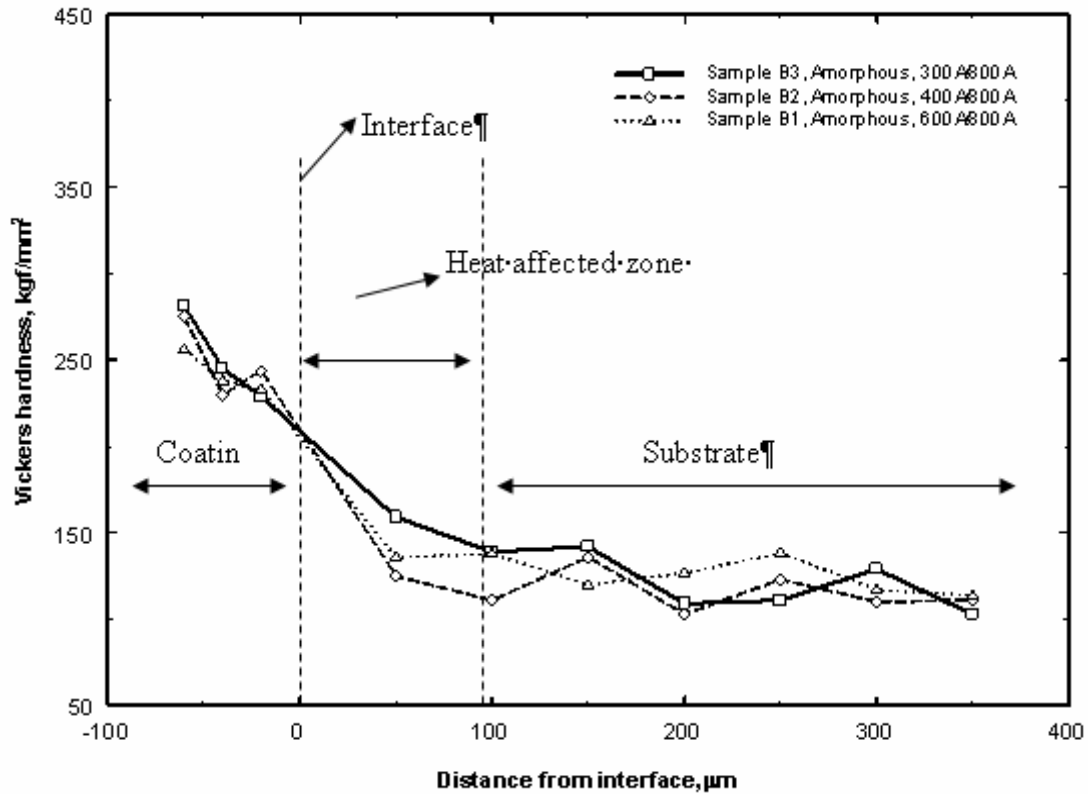


Figure 23. Microhardness profile of Sample B1, B2 and B3

The microhardness was also enhanced by amorphous coatings, as indicated in Figure 23. The highest coating microhardness value occurred with Sample B3. It was also noted that the differences in coating hardness with the three amorphous coatings were not significant. Another observation from the microhardness profile curves was that the microhardness of WC coatings is higher than that of the amorphous coatings. There are two reasons for that. One was that the hard WC precipitations enhanced the WC coating hardness. The other was related to the defects and pores in the amorphous coatings formed during thermal spray and following HDI fusing.

It has been noticed that the microhardness values exhibited fluctuations during measurement. This is mainly caused by the heterogeneity of materials (discrete distribution of WC in Fe-matrix for WC coatings and presence of porosity /voids in amorphous coatings). Other factors such as the equipment accuracy, methods etc. may also contribute to the fluctuations in microhardness.

Using the same procedures, the microhardness profiles of Sample Y1, Y2 and Y3 were obtained and are shown in Figure 24. The surface hardness enhancement similar to WC coatings was achieved for the amorphous coatings on screen sections. The three hardness regions were low hardness substrate ASTM A36 steel, high hardness amorphous coating and the moderate interface referred to as heat affected zone. Sample Y3 had the highest hardness of these three coatings. The hardness of the coating increased up to 700 kgf/mm² which was three times higher than that of the substrate. Sample Y1 showed less significant hardness enhancement that is only twice harder than the ASTM A36 steel.

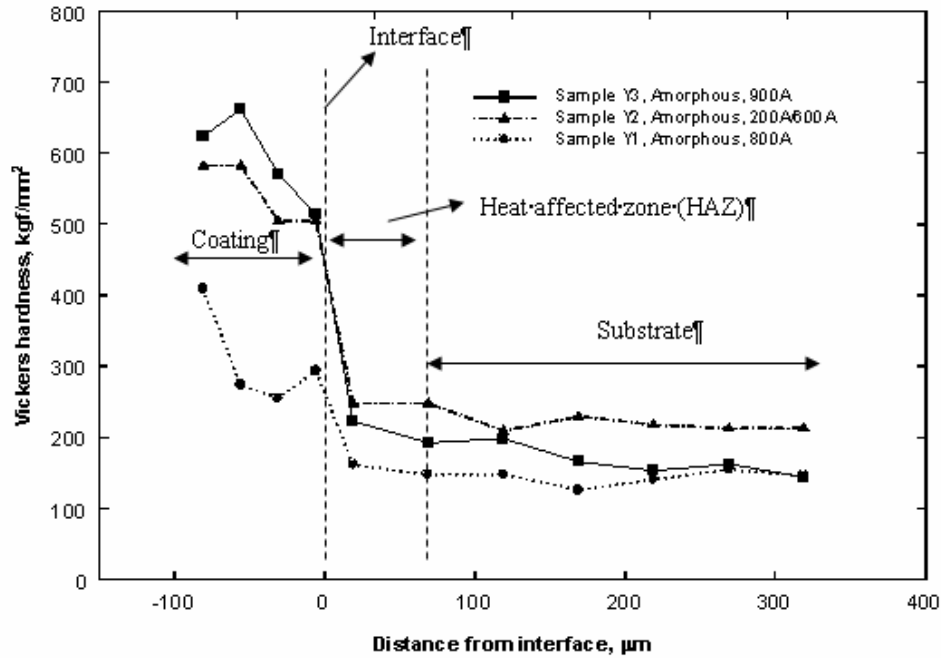


Figure 24. Microhardness profile of Sample Y1, Y2 and Y3

Wear Testing

Block-on-disk wear test was adopted to evaluate the wear resistance of all the coatings processed by HDI coating technology. During the block-on-disk tests, the weight loss with respect to the wear test duration for each specimen was recorded and shown in Figure 25, 26. The wear resistance properties of all the coated specimens were better than that of uncoated AISI 4140 steel. Of all WC coatings, Sample A3 showed the highest wear resistance and Sample B2 had the best wear resistance in the amorphous coating group. Comparing Sample A3 with Sample B2 indicates that A3 had a higher wear resistance. It seems that WC coatings were more effective in enhancing the wear resistance of AISI 4140 steel than amorphous coatings.

Wear rate is determined by plastic deformation and material removal of the specimen surface. Better wear resistance would result in lower surface plastic deformation rate. Hardness plays an important role in the wear resistance behavior.

Typically, harder surface leads to less deformation. For example, Sample A3 showed the best wear resistance in the block-on-disk wear test, which also had the highest microhardness among WC coatings. Sample B2 and B3 had the similar microhardness and wear resistance which were significantly higher than those of Sample B1. The pores observed on the SEM images may also have effects on their hardness and wear resistance.

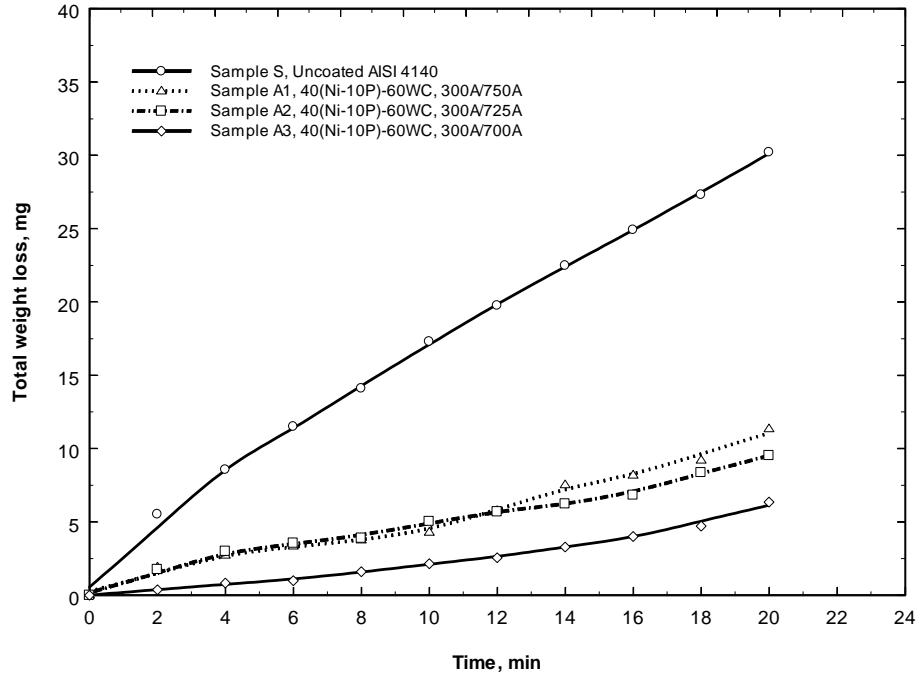


Figure 25. Block-on-disk wear test results of AISI 4140 steel with WC coatings for Sample A1, A2 and A3

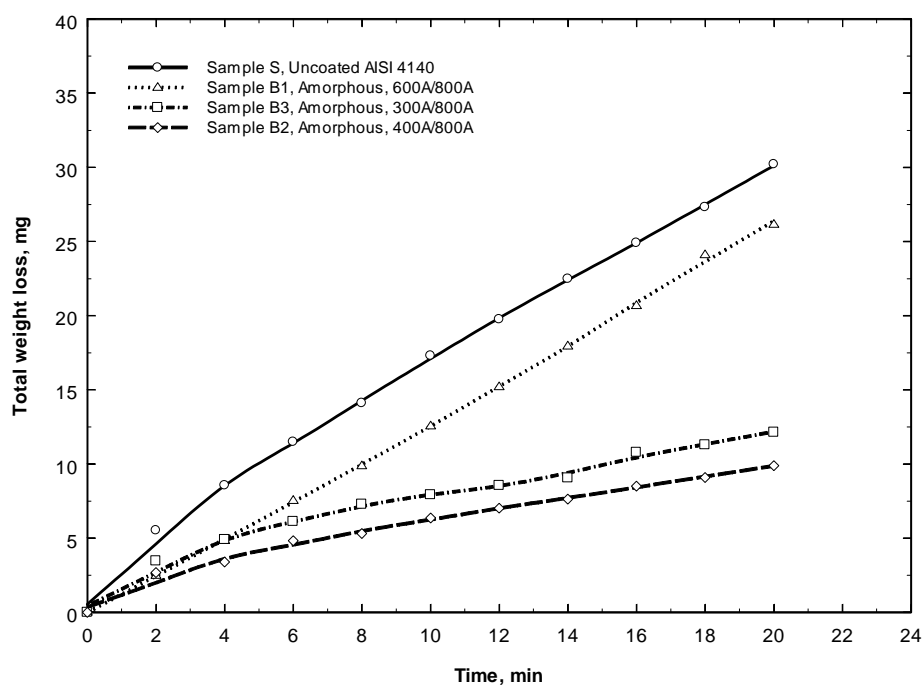


Figure 26. Block-on-disk wear test results of AISI 4140 steel with amorphous coatings for Sample B1, B2 and B3

Block-on-disk wear tests were also performed with the specimens prepared from Sample Y1, Y2 and Y3 using the same parameters and procedures. The wear results are shown in Figure 27. Sample Y1 had a very high wear rate. The reason for that is believed to be the high porosity and weak bonding of Sample Y1. The loose coating wore faster against the hard disk and even peeled off by the disk. The wear performance was worse than ASTM A36 steel, which means Sample Y1 coating can not enhance the wear performance of the screen section. Sample Y3 had a low porosity and high hardness on the coating, which helped Sample Y3 perform very well in the block-on-disk wear test.

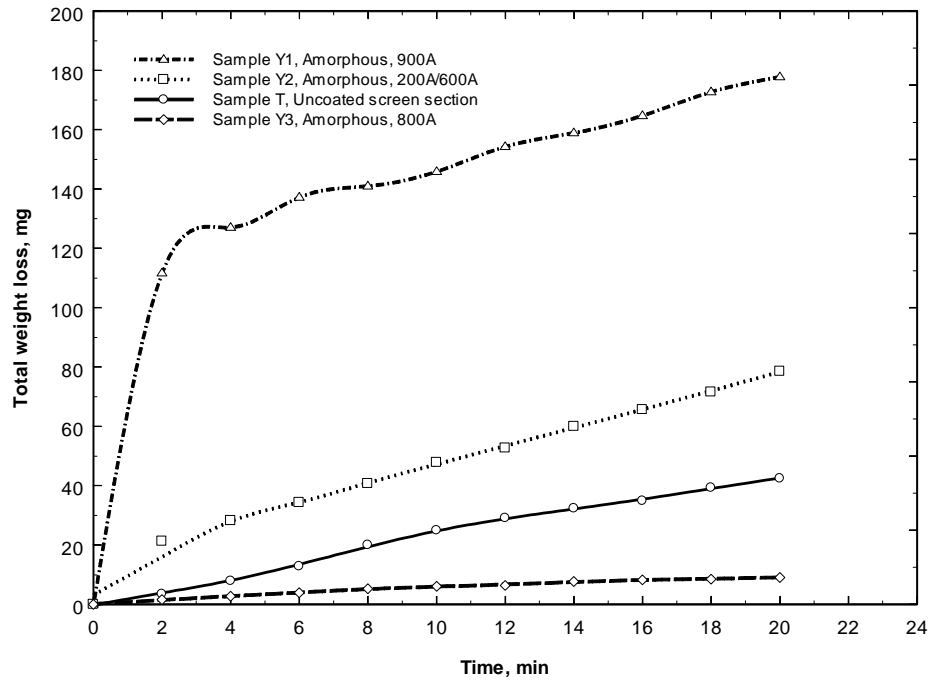


Figure 27. Block-on-disk wear test results of ASTM A36 screen section with amorphous coatings for Sample Y1, Y2 and Y3

As discussed earlier that sliding wear dominates during screening process which means the wear test method employed in this research is a suitable way to simulate the wear conditions. Additionally, the ring's rotating speed in this test, about 880 cm/s, was considerably higher than the travel speed of coal particles on the screen surface, which is usually 10-20 cm/s. Besides, the normal load of 4.54 kg is applied on the small contact area of the test specimen. All this will help to create a rapid wear rate of the specimen.

CONCLUSIONS

HDI coating technology was successfully applied in surface enhancement of mineral processing components. Two substrate materials of AISI 4140 steel and ASTM A36 screen sections, and two coating materials of (Ni-10P)-60WC and Fe-15Cr-14Mo-2Y-15C-6B, wt% were investigated. High density infrared (HDI) coating technology was adopted to process the coatings on the substrate. Two passes of fusing current including 200A, 300A, 400A and 600A for preheating pass and 600A, 700A, 725A, 750A, 800A and 900A for fusing pass were applied to achieve the coatings with different characteristics. After the HDI process, specimens were prepared for a series of characterization studies, including optical microscopy and scanning electron microscopy for the microstructural examination, microhardness testing for hardness characterization, and finally the block-on-disk wear tests to measure the wear performance of the HDI processed coating.

The following conclusions can be drawn based on the results obtained from the study:

1. Wear mechanisms of typical mineral processing equipment were identified.
2. Surface coatings with refined microstructural features were obtained by using HDI coating process.
3. SEM characterization showed the HDI coatings were metallurgically bonded to the substrates.
4. The hardnesses of both WC and amorphous coatings are higher than that of substrate materials. The hardness of WC coating was up to three times higher than that of AISI 4140 steel and amorphous coating also achieved a three times higher hardness with the ASTM A36 steel.
5. Sample A3, coated with (Ni-10P)-60WC on AISI 4140 steel by HDI (10 mm/s, 300A/700A), showed the best wear resistance in the WC coating group. The wear resistance increased up to 5 times compared to uncoated AISI 4140.
6. The EDS analyses showed the presence of WC particle and WC rich-phase. The hard WC coatings significantly enhanced wear resistance of substrate AISI 4140 steel.
7. Of three amorphous coatings, Sample B2 coated with amorphous coating Fe-15Cr-14Mo-2Y-15C-6B, wt%, on AISI 4140 steel by HDI (10 mm/s, 400A/800A) showed the best wear resistance. The wear life of AISI 4140 steel increased about 3 times by this amorphous coating.
8. For screen substrate, Sample Y3 coated with amorphous coating Fe-15Cr-14Mo-2Y-15C-6B, wt%, by HDI (10 mm/s, 800A) had the best wear resistance. The wear life of this coated materials increased about 5 times than the uncoated screen.
9. High porosity was observed with most HDI-processed coatings which adversely affected coating performance, e.g., Sample Y1, Y2 etc.
10. In the HDI process, two scanning passes are preferred to wet the coating first and then fuse at higher current to produce strong bonding and high density, high hardness coating.

REFERENCES

- Agarwal, A. and Dahotre, N. B., 2000, "Comparative wear in titanium diboride coatings on steel using high energy density processes," *Wear*, v 240, n 1-2, pp 144-151
- Ahn, S.H., Lee, J.H., Kim, H.M. and Kim, J.G., 2004, "A study on the quantitative determination of through-coating porosity in PVD-grown coatings," *Applied Surface Science*, 233 (1-4), pp. 105-114.
- Blue, C.A., Sikka, V.K., Ohriner, E.K., Engleman, P.G. and Harper, D.C., 2000, "High-density-infrared transient liquid coatings," *JOM-e*, 52(1) <http://www.tms.org/pubs/journals/JOM/0001/Blue/Blue-0001.html>.
- Blue, C. and Sikka, V., 2000, "Infrared transient-liquid-phase coating of materials," *Proceedings of the 7th PEWG Meeting*, July 17-20.
- Blue, C.A., 2002, "High-Intensity lamp opening new surface-treating vista," *Industrial Heating*, 69(3), p. 79(4).
- Davis, J.R.(Ed), 1998, *Metals Handbook*, 2nd edition; ASM International, Materials Park, OH, USA.
- Dunn, D.J., 1985, "Metal removal mechanisms comprising wear in mineral processing," *Proceeding of International Conference on wear of Materials*, April 14-18, Vancouver, BC, Canada
- Durman, R.W., 1988, "Progress in abrasion resistant materials for use in comminution processes," *International Journal of Minereral. Processing*, pp. 381-399
- Engleman, P.G., Dahotre, N.B., Blue, C.A., Harper, D.C. and Ott, R., 2002, "High density infrared processing of WC/Ni-11P composite coatings," *Surface Engineering*, 188(2), pp. 113-119.
- Foster, J., 1996, "Ceramic applications for wear protection of pipe lines and cyclones," *Key Engineering Materials*, 122-124, pp. 247-278.
- Khedkar, J.; Khanna, A.S. and Gupt, K.M., 1997, "Tribological behaviour of plasma and laser coated steels," *Wear*, v 205, n 1-2, pp 220-227
- Laurila, M.J. and Budge, G., 2000, "Benchmarking coal prep practice: An Update," *Proceedings of 17th International Coal Preparation Exhibition & Conference*, Lexington, KY, USA, pp. 51-55.
- Leonard. J. W. and Hardinge, B.C., 1991, *Coal preparation*, 5th edition, Society for Mining, Metallurgy and Exploration, Inc., Littleton, CO, p 223.
- Mining Journal Ltd., 1999, *Mining Annual Review*
- Muralidharan, G.; Blue, C.A.; Sikka, V.K.; Dahotre, N.B., 2004, "Surface modification of 4340 steel with iron aluminides using high-energy-density processes," *Materials Science and Technology*, v 2: AIST/TMS Proceedings, pp 357-366

- Norman, T.E., 1980, "Wear in ore processing machinery," in: *Wear Control Handbook* Peterson, M.B. and Winor, W.O. (Eds.), ASME, pp. 109–115
- Nonnen, F.A., 1985, "Wear resistant materials reduce costs," *Bulk Solids Handling*, 5(5), pp. 1035-1039.
- Raghunath, C.; Bhat, M.S.; Rohatgi, P.K. 1995, "In situ technique for synthesizing Fe-TiC composites," *Scripta Metallurgical Material*, v 32, n 4, pp. 577-582
- Watson, J; Mutton, P.; Sare, I., 1980, "Abrasive wear of white cast irons," *Metals forum*, v3, n 1. pp55
- Wills, B.A., 1985, *Mineral Processing Technology*, 3rd edition: An Introduction to the Practical Aspects of Ore Treatment and Mineral Recovery, Pergamon Press, Oxford, England, p.238, pp. 232-235.
- Wu, P., Zhou, C.Z. and Tang, X.N., 1995, "Laser alloying of a gradient metalceramic layer to enhance wear properties," *Surface & Coatings Technology*, 73 (1-2), pp. 111-114.
- Xu, L., Vose, C. and StJohn, D., 1993, "Abrasive wear of study of selected white cast irons as liner materials for the mining industry," *Wear*, 162-164(part 2), pp. 820-832.
- Wu, P., Du, H.M., Chen, X.L., Li, Z.Q., Bai, H.L. and Jiang, E.Y., 2004, "Influence of WC particles behavior on the wear resistance properties of Ni-WC composite coatings," *Wear*, 257(1-2), pp. 142-147.